SOLVING THE CONUNDRUM OF MASS RECRUITMENT BY SMALL ANT COLONIES

ROBERT PLANQUÉ, JAN BOUWE VAN DEN BERG, AND NIGEL R. FRANKS

ants; social insects; recruitment; differential equations; collective behaviour; behavioural ecology

Abstract. Large ant colonies invariably use effective scent trails to guide copious ant numbers to food sources. The success of mass recruitment hinges on the involvement of many colony members to lay powerful trails. However, many ant colonies start off as single queens. How do these same colonies forage efficiently when small, thereby overcoming the hurdles to grow large? In this paper, we study the case of combined group and mass recruitment displayed by some ant species. Using mathematical models, we explore to what extent early group recruitment may aid deployment of scent trails, making such trails available at much smaller colony sizes.

1. Introduction

Mass recruitment, the use of scent trails to guide nest mates to food sources, is synonymous with the ecological success of many ant colonies (Beckers et al., 1989; Hölldobler and Wilson, 1990; Franks et al., 1991). Yet many ant colonies are founded by single queens (Buschinger, 1974; Hölldobler and Wilson, 1977; Bourke and Franks, 1995). So how do such tiny colonies ever forage sufficiently successfully to build up their worker populations so that they can take full advantage of mass recruitment? In other words, how do small colonies manage to forage reliably? Our aim here is to begin to solve this conundrum.

Reliability in animal communication is paramount (Wilson, 1975), particularly for animals living together in tightly knit groups. Visual cues, such as the distinctive patterns on fish, serve to keep the the schools or flocks together (Katzir, 1981; Tayssedre and Moller, 1983). Howling of wolves serves in part the same purpose (Harrington and Mech, 1979). Directing flocks to particular targets is robust, in the sense that larger groups need relatively fewer leaders to direct it (Couzin et al., 2005).

Social insects go one step further: they recruit colony members to food sources in a variety of ways, thereby increasing the yield from their collective foraging (Wilson, 1971; Oster and Wilson, 1978). Those who have found food (either independently or through information provided by nest mates (Dechaume-Moncharmont

et al., 2005)) need to inform naive nest mates to create a positive feedback loop, so that over time much of the colony is aware of the food and may act upon this information. A famous example is the honeybees' waggledance which is used to encode several aspects of a food source to colony members at the hive, such as quality, distance, and the direction in which the food can be found (Haldane and Spurway, 1954; von Frisch, 1967). All such recruitment methods need to be reliable, in particular under changes in colony composition. Ants, especially, often start colonies as single queens but grow to thousands or even millions over the course of the colony's lifespan (Hölldobler and Wilson, 1990, 2009). All this time, the colony has to rely on its recruitment methods for efficient food collection.

Ants, in general, employ a large variety of recruitment methods to relay information on food or nest sites. In two such methods, tandem running and group recruitment, a leader ant guides a single ant or a small group of ants to a recruitment target such as a food source or a new potential nest. We will refer to these two types of recruitment as 'group recruitment' (GR) throughout. This flies in the face of convention (Beckers et al. 1989—which distinguishes tandem running from group recruitment) but we do it both for simplicity and clarity and because a group of two, albeit small, is still a group.

The speed at which group recruitment proceeds is intrinsically limited by the number of leader ants active at any moment, making it rather slow. A prime benefit of this individual-based recruitment, however, is that it works well also when numbers of ants are small. In principle, two ants, one leading and one following, suffice. The probability of such a recruitment event succeeding does not improve when more ants are actively recruiting.

Ants use various other recruitment methods, all involving scent marking (Hölldobler and Wilson, 1990). Pheromone trails (PT) are well-known to be very efficient in guiding large numbers of ants to a target. Once a trail is established, recruitment by such scents is highly effective since the trail allows reliable direct navigation between the nest and the recruitment target. Some trails may last for hours or even days, thus freeing the ants who have laid the trail to be active elsewhere (Robinson et al., 2005; Jackson et al., 2006; Jackson and Ratnieks, 2006). The major downfall of this method is precisely when numbers of ants are small: the trail is then laid down too slowly to overcome evaporation. As a consequence, trails are not strong enough to guide ants reliably to a target (Britton et al., 1998).

Intriguingly, in some ant species, such as *Tetramorium* (Hölldobler and Wilson, 1990), the use of trails is preceded by an initial phase of group recruitment or tandem running. Recent work by Collignon and Detrain (2010) has shown that this two-stage group-mass recruitment method allows these ants to make better choices than when group recruitment is experimentally prohibited.

Here we suggest that another reason why this early group recruitment is used is to allow for the actual use of pheromone trails at all. It has been known for some

time that ant colonies need to have a certain minimum size in order for pheromone trails to be used (Beckers et al., 1989; Beekman et al., 2001; Planqué et al., 2010). *Tetramorium* species have colonies of moderate size (Brian et al., 1967; Brian and Elmes, 1974), and it may be difficult to establish powerful scent trails with rather few ants. In the early stages of recruitment to a food source, trails are laid but are not much used by the workers (Collignon and Detrain, 2010). The chances of losing a weak trail are indeed great (Deneubourg et al., 1983). Here we investigate using mathematical models whether an early bout of a more individual type of recruitment may lessen this burden of high minimum colony size and make scent trails available to ants with smaller colony sizes as well.

2. Modeling

The following equations describe the build up of recruiter numbers after a site with food has been discovered by a few scouts. A typical time scale at which the dynamics take place is a few hours. We consider a colony of ants of size N, in which individual workers are able to recruit using both GR and PT methods. In other words, workers are able both to lead single ants or small groups to a food source and to lay down and follow scent trails. Ants are assumed to be able to use either recruitment method at any moment exclusively.

In this model, $p(t)$ denotes the number of ants using pheromone trails and $l(t)$ is the number of ants involved in group recruitment, leaving $N - l - p$ ants not involved in either recruitment method. Ants following or leading tandem runs or groups are able to build up a trail which may be used at some later time when recruiter numbers are sufficient. Hence, we need to take the dynamics of pheromones explicitly into account. In the following, c_i, $i = 1, \ldots, 8$, are positive rate constants.

Let $q(t)$ be the amount of pheromone on trails at time t. Then we model the build up of ants following scent trails as follows,

$$\frac{dp}{dt} = c_1 q(N - l - p) - \frac{c_2 p}{c_3 + q}. \tag{1}$$

This equation involves a simple positive feedback mechanism, in which trail strength q interacts with uncommitted workers $N - l - p$, and a loss term which incorporates that the per capita probability to lose the trail $c_2/(c_3 + q)$ depends on the strength of the trail. Using the number of ants on the trail as a proxy for the trail's strength, we find

$$\frac{dp}{dt} = \tilde{c}_1 p(N - l - p) - \frac{\tilde{c}_2 p}{\tilde{c}_3 + p},$$

using a slightly different definition for constants $\tilde{c}_1$, $\tilde{c}_2$ and $\tilde{c}_3$, as used in previous models (Beekman et al., 2001; Planqué et al., 2010). The pheromones are assumed to be laid down by ants $l(t)$ involved in group recruitment, or by ants following

trails $p(t)$. In both cases, the scent is laid when returning from a recruitment target. Adding moreover degradation of the trail, the concentration of scent over time satisfies

$$\frac{dq}{dt} = -c_4 q + c_5 l + c_6 p. \tag{2}$$

There are two natural choices for c_5: either GR ants, l, do not contribute at all, in which case $c_5 = 0$, or they contribute as much to the trail as PT ants p, and we set $c_5 = c_6$. We will restrict our analysis to $0 \leq c_5 \leq c_6$, and both limit cases will be studied in detail. The build-up of ants involved in GR is modelled as follows,

$$\frac{dl}{dt} = c_7 l(N - l - p) - c_8 l. \tag{3}$$

This equation combines the same simple positive feedback between recruiter ants and the inactive part of the colony as in (1) with a per capita constant loss term: the per capita probability for a GR act to succeed does not depend on the number of GR ants involved.

Equations (1)–(3) form the main model analysed in this paper. The initial conditions we prescribe are $(p, q, l)(0) = (p_0, 0, l_0)$, with p_0 small and possibly zero, and l_0 small but positive to signify the start of a recruitment event.

The main questions we pose to this model are

- Which steady states does this model possess?
- What are their stability properties? In particular, which steady state is an attracting one starting from the given initial conditions, and how does this change when colony size is changed?
- Whilst changing colony size, are there any new equilibria in which pheromones are used?
- Can we understand the transitions from GR to PT, as colony size increases?
- How do the minimum colony sizes to use PT compare between the two important cases, $c_5 = 0$ and $c_5 = c_6$? Are scent trails accessible for smaller colonies if they use a group-mass recruitment system?

Before diving straight into the analysis, we present an overview of the results, to give the reader some intuition of the more detailed discussion to follow.

Depending on parameter settings, we find between one and five steady states. If GR ants do not contribute to trails, the dynamics is analogous to the model analysed in (Planqué et al., 2010). We find three potentially stable steady states: the trivial one (neither recruitment strategy), a PT equilibrium and a GR equilibrium. A separatrix marks the boundary between the domains of attraction. For both recruitment steady states, colony size N should be sufficiently large to be attracting for solutions starting near the origin. As N increases starting from some small value, the dynamics first converge to GR and for larger values to PT. This is expounded in Section 4.

The main question thus becomes if the minimum colony size to reach a PT equilibrium is reduced if GR ants do contribute to trails. The analytically tractable (and biologically most interesting) case when GR ants deposit scent at a rate equal to PT ants ($c_5 = c_6$) is studied in detail in Section 5. In this case, the GR-only equilibrium is replaced by a mixed steady state which can indeed be stable and attracting. A local stability analysis of this mixed steady state, however, shows that when c_2 is small enough (i.e., when the probability to lose the scent trail is low), the transition from a mixed equilibrium to trails involves a Hopf bifurcation followed by a heteroclinic cycle. The biological consequence is that the transition to effective scent trails is made at a lower colony size. To get a better insight into the emergence of this phenomenon, we unfold the Hopf bifurcation in the two limiting cases, when $N_{\min} \lesssim N_{\max}$ and $\hat{N} \lesssim N_{\max}$ using regular perturbation expansions (Sections 8.1 and 8.2). The particular colony size values $N_{\min}$ and $N_{\max}$ span the colony range for which the mixed equilibrium exists, and $\hat{N}$ is the minimum colony size for the PT equilibrium. In the first limiting case, the Hopf bifurcation coincides with the heteroclinic cycle; in the second case, the Hopf bifurcation can be analyzed, but the heteroclinic cycle remains beyond our grasp.

The detailed insight gained from the $c_5 = c_6$ case is finally put into a more complete picture by studying model for intermediate values $0 < c_5 < c_6$ using numerical experiments (Section 6). The Hopf bifurcation and subsequent heteroclinic cycles are shown to be robust phenomena (for small c_2). Most importantly, the analytical results show how the different parts of the recruitment mechanisms may contribute to facilitate a transition from mixed strategies to only scent trails. A combination of a low net deposition rate of trail scent and good GR recruitment build up should give the greatest benefit of using GR to build efficient scent trails.

3. Steady states

Without loss of generality, we may set $c_1 = 1$ by rescaling time. We define a number of parameter combinations, which will be used throughout the paper. Let us set

$$\alpha = \frac{c_6}{c_4}, \quad \beta = \frac{c_8}{c_7}, \quad \gamma = \frac{c_8}{c_7 c_2}(c_6 - c_5).$$

Equilibria are first given as pairs (l, p), with q to be determined. We find two pairs, $(\hat{p}, \hat{l})$ and $(\bar{p}, \bar{l})$. For the first of these,

$$\hat{p} = \frac{1}{\alpha}\hat{q}, \quad \hat{l} = 0.$$

The pheromone trail at steady state satisfies either $\hat{q} = 0$, in which case we find the trivial steady state, denoted P_1, or $\hat{q} = \hat{q}_\pm(N)$ where

$$\hat{q}_\pm(N) = \frac{\alpha N - c_3}{2} \pm \frac{1}{2}\sqrt{(c_3 + \alpha N)^2 - 4c_2}. \tag{4}$$

The two resulting steady states,

$$P_2 = (p_2, q_2, l_2) = (\frac{\hat{q}_+}{\alpha}, \hat{q}_+, 0), \quad P_3 = (p_3, q_3, l_3) = (\frac{\hat{q}_-}{\alpha}, \hat{q}_-, 0),$$

involve only ants following trails at steady state. This pair of equilibria forms a continuous family in N, and we will sometimes refer to the complete family as $P_{23}(N)$.

The second pair $(\bar{p}, \bar{l})$ satisfies

$$\bar{p} = \frac{\beta}{c_2}\bar{q}(c_3 + \bar{q}), \quad \bar{l} = N - \beta - \frac{\beta}{c_2}\bar{q}(c_3 + \bar{q}).$$

We can interpret β as the number of ants not involved in recruitment at the mixed steady state, since $\beta = N - \bar{l} - \bar{p}$. At these steady states, $\bar{q}$ solves

$$\gamma\bar{q}^2 + (c_3\gamma - c_4)\bar{q} + c_5(N - \beta) = 0, \tag{5}$$

with solutions $q_4(N) < q_5(N)$ if $\gamma \neq 0$ (i.e., if $c_5 \neq c_6$), giving rise to two mixed steady states, P_4 and P_5. These form again a continuous family in N, and will sometimes be denoted by $P_{45}(N)$. In the important case $c_5 = c_6$, i.e., $\gamma = 0$, we find only one steady state, P_4, in which

$$q_4 = \alpha(N - \beta).$$

Figure 1 illustrates how the q component of the different steady states vary with N.

3.1. **Existence of equilibria.** The pheromone-only steady states $P_{23}(N)$ exist only if N is large enough for the discriminant in $\hat{q}_\pm(N)$ to be positive, so when

$$N \geq \hat{N} := \frac{2\sqrt{c_2} - c_3}{\alpha}.$$

For the mixed steady states, let us first assume that $\gamma = 0$. The mixed equilibrium P_4 is biologically relevant if $N \in [N_{\min}, N_{\max}]$, where

$$N_{\min} := \beta, \quad N_{\max} := \beta - \frac{c_3}{\alpha} + \frac{c_2}{\alpha^2\beta}.$$

At $N = N_{\max}$, $\bar{l} = 0$, and the steady state is thus of the form $(p_4, q_4, 0)$, and P_4 in fact coincides with P_2 or P_3 here, depending on the other parameter values. A prerequisite for $N_{\max} > N_{\min}$ is that

$$-\frac{c_3}{\alpha} + \frac{c_2}{\alpha^2\beta} > 0 \quad \Longleftrightarrow \quad \alpha\beta < \frac{c_2}{c_3} \quad \Longleftrightarrow \quad \frac{c_8}{c_7}\frac{c_6}{c_4}\frac{c_3}{c_2} < 1. \tag{6}$$

We will assume this throughout, and many results depend on it. The reason to assume (6) is that we are particularly interested in how a colony using, at least in part, individual-based recruitment methods, makes the transition to using trails only as colony size increases. Mathematically, this amounts to a transition from

orbits converging to a stable attracting steady state P_4 to orbits converging to P_2 or P_3. The existence of P_4 is thus essential and is guaranteed by assuming (6).

If $\gamma \neq 0$, we find two steady states, P_4 and P_5. The roots $\bar{q}$ of (5) exist if

$$N \leq N_{\mathrm{SN}} := \beta + \frac{(c_3\gamma - c_4)^2}{4\gamma c_5}.$$

The q-component of the P_{45} equilibria, $\bar{q}(N)$, becomes positive at $N = N_{\min}$ and the l-component vanishes at $N = N_{\max}$. However, if $q_4(N_{\mathrm{SN}}) < q_4(N_{\max})$, then the steady states are biologically relevant for $N \in [N_{\min}, N_{\mathrm{SN}}]$.

Studying the stability of these steady states, especially of the mixed ones P_4 and P_5, proves difficult. However, the cases $c_5 = 0$, when GR ants do not contribute to scent trails, and $c_5 = c_6$, when GR and PT ants contribute equally, are accessible and shed much light on the equilibria at intermediate values of c_5. We will now study the two limit cases in turn, and then study the intermediary case $0 < c_5 < c_6$.

4. GR ants do not contribute to scent trails: the case $\mathbf{c_5 = 0}$

Let us assume that group recruiting ants do not contribute to scent trails and set $c_5 = 0$, and consider

$$\frac{dp}{dt} = q(N - l - p) - \frac{c_2 p}{c_3 + q}, \tag{7}$$

$$\frac{dq}{dt} = -c_4 q + c_6 p, \tag{8}$$

$$\frac{dl}{dt} = c_7 l(N - l - p) - c_8 l. \tag{9}$$

Apart from the steady states P_1, P_2 and P_3, which do not depend on c_5, there are two steady states in which GR ants are present. In one, $P_4 = (0, 0, N - \beta)$, they feature exclusively, and the other, P_5, is a fully mixed steady state.

The model above closely matches one studied previously in detail in Planqué et al. (2010). The main differences with the current model is that pheromones were not taken into account explicitly, and that in group recruitment a distinction was made between ants leading and following in tandem groups. In that model, there are also five equilibria, and there is a qualitative one-to-one correspondence to the five steady states above. Moreover, the stability properties are qualitatively the same, when varying colony size N.

In this paper, we are chiefly concerned with the stability of steady states in which ants follow trails, and for which solutions starting close the origin converge to such scent equilibria. In Planqué et al. (2010) it was shown that solutions starting close to the origin can only converge to the scent equilibrium P_2 if the other of the pair, P_3, which is always unstable when biologically relevant, has

passed the origin. This happens at

$$N = N_3 := \frac{c_2}{\alpha c_3}.$$

The same is true in model (7)–(9). The only fully mixed steady state, P_5, which appears in both models, is unstable whenever it is biologically relevant.

We thus conclude that, as in Planqué et al. (2010), colony sizes need to be sufficiently large for P_3 to pass the origin, before the only stable steady state containing ants following trails, P_2, becomes attracting for solutions starting near the origin.

How does this result change when ants involved in GR or TR lay down trail as well? The major part of the rest of this paper studies the other natural choice for parameter c_5: $c_5 = c_6$.

5. GR ants contribute fully to scent trails: the case $\mathbf{c_5 = c_6}$

The second case for which the dynamics may be studied analytically in more detail is when ants following trails contribute as much pheromone to these trails as ants leading tandems or groups, reflected in $c_5 = c_6$:

$$\frac{dp}{dt} = q(N - l - p) - \frac{c_2 p}{c_3 + q}, \tag{10}$$

$$\frac{dq}{dt} = -c_4 q + c_6(l + p), \tag{11}$$

$$\frac{dl}{dt} = c_7 l(N - l - p) - c_8 l. \tag{12}$$

This model has one less steady state than the full model: it features P_1, the origin, two trail equilibria involving no leader ants, P_2 and P_3 as before, and one (rather than two, when $c_5 \neq c_6$) mixed equilibrium in which leader ants and pheromone trails are used, $P_4 = (p_4, q_4, l_4)$, where

$$p_4 = \frac{\alpha\beta}{c_2}(N - \beta)(c_3 + \alpha(N - \beta)) \tag{13}$$

$$q_4 = \alpha(N - \beta), \tag{14}$$

$$l_4 = N - \frac{\alpha\beta}{c_2}(N - \beta)(c_3 + \alpha(N - \beta)) - \beta. \tag{15}$$

In the following sections, we give a detailed description of the behaviour of solutions for this model, where we use colony size N as the main "bifurcation" parameter.

The analysis of the steady states starts with a local stability analysis of the equilibria. Recall the following critical values for N,

$$N_{\min} = \beta, \quad \hat{N} = \frac{2\sqrt{c_2} - c_3}{\alpha}, \quad N_{\max} = \beta - \frac{c_3}{\alpha} + \frac{c_2}{\alpha^2\beta}.$$

5.1. **Local stability of P_2 and P_3.** Equilibria P_2 and P_3 are of the form $(\hat{p}, \hat{q}, 0)$. At such a steady state, the Jacobian is given by

$$J := \begin{pmatrix} -A & B & -\hat{q} \\ c_6 & -c_4 & c_6 \\ 0 & 0 & c_7(N - \hat{p} - \beta) \end{pmatrix},$$

where

$$A = \hat{q} + \frac{c_2}{c_3 + \hat{q}}, \quad B = N - \hat{p} + \frac{c_2\hat{p}}{(c_3 + \hat{q})^2}.$$

One of the eigenvalues is hence $c_7(N - \hat{p} - \beta)$. It passes through zero at $N = N_{\max}$, which may be seen as follows. At $N = N_{\max}$, the l-coordinate of P_4 vanishes, and $q_4 = \hat{q}_+$ or $q_4 = \hat{q}_-$, depending on the ordering of $q_4(\hat{N})$ and $q_{23}(\hat{N})$. Hence, in the case of the first ordering, $P_2 = P_4$ at this value of N, and in the second case, $P_3 = P_4$. But since $l_4 = N - p_4 - \beta$, the eigenvalue $c_7(N - \hat{p} - \beta)$ is zero at $N = N_{\max}$.

At $\hat{N}$ there is a saddle-node bifurcation at which the two branches of equilibria P_2 and P_3 appear. Here, one eigenvalue of J passes through zero, the other being negative. To see this, let

$$J_s := \begin{pmatrix} -A & B \\ c_6 & -c_4 \end{pmatrix},$$

be the relevant submatrix of the Jacobian, whose eigenvalues determine the stability of solutions near $\hat{N}$. The characteristic equation is

$$(-A - \lambda)(-c_4 - \lambda) - c_6 B = \lambda^2 + (A + c_4)\lambda + Ac_4 - c_6 B = 0, \tag{16}$$

and we note that the trace is always negative. The stability changes when the determinant of J_s vanishes. Along the branch $P_{23}(N)$, q and N satisfy

$$\hat{q}(N - \hat{q}/\alpha) = \frac{c_2\hat{q}/\alpha}{c_3 + \hat{q}}.$$

Note that $\hat{q} > -c_3$ for any $N \geq \hat{N}$. The nontrivial solution for q satisfies

$$(\alpha N - \hat{q})(c_3 + \hat{q}) = c_2,$$

which is the same as

$$N = \frac{1}{\alpha}\Big(\frac{c_2}{c_3 + \hat{q}} + \hat{q}\Big).$$

If we plug this into the determinant of J_s, we find

$$\det J_s = \hat{q}\Big(\frac{(c_3+\hat{q})^2 - c_2}{(c_3+\hat{q})^2}\Big),$$

so that $\det J_s = 0$ either when $\hat{q} = 0$ or when $(c_3+\hat{q})^2 = c_2$. On $(-c_3, \infty)$, this equation has only one solution, $\hat{q} = \sqrt{c_2} - c_3$. As we have seen, the determinant of J_s changes sign precisely at the saddle-node. Starting at low $\hat{q}$ values on the P_3 branch, the determinant is negative, and P_3 is hence unstable. Conversely, P_2 has three stable eigenvalues.

5.2. **Local stability of P_4.** Steady state P_4 may change stability through a transcritical bifurcation, in which an eigenvalue passes through the origin, or via a Hopf bifurcation, in which a pair of eigenvalues passes through the imaginary axis. We will show that the latter occurs if

$$c_2 < c_2^* := \alpha^2\beta^2. \tag{17}$$

Whether it also occurs when $c_2 > c_2^*$ is not straightforward, but we conjecture that it does not. All numerical results indicate that it does not and that P_4 is locally stable in this case. It is at least clear that P_4 cannot lose stability through a simple eigenvalue through the origin, by the following argument.

Along the branch of equilibria $P_4(N)$, the Jacobian has the form

$$J = \begin{pmatrix} -A(N) & B(N) & -q_4(N) \\ c_6 & -c_4 & c_6 \\ -D(N) & 0 & -D(N) \end{pmatrix},$$

where A, B and D are positive functions of N given by

$$\begin{aligned} A(N) &= q_4(N) + \frac{c_2}{c_3 + q_4(N)}, \\ B(N) &= \beta + \frac{\beta q_4(N)}{c_3 + q_4(N)}, \\ D(N) &= c_7 l_4. \end{aligned}$$

The characteristic equation is thus given by

$$-\lambda^3 + (-A - c_4 - D)\lambda^2 + (D(q_4 - c_4 - A) + c_6 B - c_4 A)\lambda + Dc_4(q_4 - A) = 0.$$

The determinant of J, $Dc_4(q_4 - A)$, only changes sign when $q_4 = A$. Since $D > 0$ whenever P_4 is biologically relevant, this is equivalent to $A = 0$, which occurs when $l_4 = 0$, i.e., at $N = N_{\min}$ and $N = N_{\max}$.

Inequality (17) is also equivalent to an ordering of q values. The trail-only steady states P_2 and P_3 exist for $N \geq \hat{N}$. Let us denote the single scent-only steady state at $N = \hat{N}$ by $(\tilde{p}, \tilde{q}, 0)$. If $c_2 < c_2^*$ then

$$q_4(\hat{N}) > \tilde{q},$$

and the intersection between P_4 and P_{23} occurs in the top branch P_2. If the ordering is the other way round, the intersection lies in the lower branch, P_3. See Figure 2.

5.3. **A Hopf bifurcation on $P_4(N)$.** We set $c_2 < c_2^*$, and focus on the pair of complex eigenvalues of $P_4(N)$. To show that a Hopf bifurcation occurs for some N between $N_{\min}$ and $N_{\max}$, we investigate when a pair of purely imaginary eigenvalues passes the imaginary axis. Consider the characteristic equation

$$-\lambda^3 + a\lambda^2 + b\lambda + c = 0.$$

Then $\lambda = i\mu$ is an eigenvalue if and only if $b = -\mu^2$ and $-ab = c$. As detailed above, $c = Dc_4(q_4 - A)$ does not have any roots for any $N \in [N_{\min}, N_{\max}]$. Since $a < 0$ for any $q > 0$, b must be negative if the equation $-ab = c$ is to be satisfied.

The resulting function $-ab - c$ is given by

$$\begin{aligned} m(N) := (A(N) + c_4 + D(N))\Big[D(N)(q_4(N) - c_4 - A(N)) \\ + c_6 B(N) - c_4 A(N)\Big] - D(N)c_4(q_4(N) - A(N)). \end{aligned} \tag{18}$$

We want to know whether $m(N)$ has a root for N between $N_{\min}$ and $N_{\max}$. A direct calculation in Maple (Version 14.00, Waterloo Maple Inc., 2010) shows that

$$m(N_{\min}) = \left(\frac{c_2}{c_3} + c_4\right)\left(c_6\beta - \frac{c_4 c_2}{c_3}\right),$$

and hence, using (6), $m(N_{\min}) < 0$. In $N = N_{\max}$, we have

$$\text{sign } m(N_{\max}) = \text{sign}\Big((\alpha^2\beta^2 - c_2)(c_2 - \alpha\beta c_3)\Big), \tag{19}$$

so that, again using (6),

$$m(N_{\max}) > 0 \qquad \Longleftrightarrow \qquad c_2 < \alpha^2\beta^2 = c_2^*.$$

So if $c_2 < c_2^*$, there is indeed a Hopf bifurcation on the P_4 branch. Let us call the value of N at which a Hopf bifurcation occurs N_H.

5.4. **A heteroclinic cycle.** Numerical analysis indicates that for some N between N_H and $N_{\max}$ there exists a cycle consisting of two heteroclinic orbits connecting the origin and the unstable P_3 steady state. The value at which this cycle occurs is denoted by N_c. For $N \in (N_H, N_c)$, orbits starting close to the origin converge onto a stable limit cycle. For $N > N_c$, such orbits converge to P_2. See Figure 3 for an example.

We cannot prove the existence of this heteroclinic cycle for all parameter values such that $N_{\min} < N_{\max}$ and $c_2 < c_2^*$. We will try to shed more light on this phenomenon using asymptotic analysis in Section 8.1 and 8.2. Note, however, that its existence is consistent with the dimensions of the stable and unstable

manifolds at the steady states that are connected. For $N > N_{\min}$ the origin has one unstable eigenvalue, and thus a one-dimensional unstable manifold. The lower branch, P_3 has a two-dimensional stable manifold. An intersection between a one-dimensional manifold and a two-dimensional one is a generic phenomenon when we vary a parameter.

5.5. **Conclusion of local stability analysis.** In all, we have found two main scenarios, characterized by the position of the rate of losing the trail, c_2 relative to $c_2^* = \alpha^2\beta^2$.

First of all, the P_2 branch is locally stable for all $N > N_{\max}$.

If $c_2 > c_2^*$, then P_2 and P_4 meet at $N = N_{\max}$, and P_4 loses a stable eigenvalue, and P_2 gains one. For $N \in (\hat{N}, N_{\max})$, P_2 is unstable. P_3 is always unstable.

If $c_2 < c_2^*$, P_4 meets P_3 at $N = N_{\max}$. Now P_2 is stable from $\hat{N}$ onwards, and P_3 is always unstable. P_4 is stable from $N_{\min}$ until the Hopf bifurcation, which occurs at $N_H < N_{\max}$. Numerics suggests that a heteroclinic cycle appears just after the Hopf bifurcation, allowing solutions starting near the origin to converge to the scent equilibrium P_2.

It is possible to obtain a deeper understanding of the solution structure by studying how the different types of solutions unfold. The Hopf bifurcation exists whenever $N_{\min} < N_{\max}$, provided that $\hat{N} < N_{\max}$. In the Appendix, we study in detail the extremal situations $N_{\min} \lesssim N_{\max}$ and $\hat{N} \lesssim N_{\max}$ using an asymptotic analysis. In the first case, both the Hopf bifurcation and the heteroclinic cycle may be found by suitable scaling arguments, and occur at the same value of N. The situation in the latter case is more subtle; the Hopf bifurcation does occur, but the heteroclinic cycle disappears by zooming in. This is to be expected, as the cycle connects steady states that are far removed from each other in state space.

6. GR ants contribute moderately to scent trails: connecting $c_5 = 0$ to $c_5 = c_6$.

When GR ants do not contribute to the pheromone trail ($c_5 = 0$), dynamics are essentially the same as in Planqué *et al.* (2010): solutions starting near the origin either converge to a GR-only steady state, or to a PT-only steady state. The mixed steady state is unstable whenever it exists and separates the basins of attraction of the two stable equilibria. Importantly, the scent trail is reachable only when the other, unstable, pheromone steady state has passed the origin.

When GR ants contribute to the scent trail at an equal rate to PT ants, $c_5 = c_6$, the GR-only steady state changes into a mixed steady state. This equilibrium only exists for intermediate colony sizes. Before or precisely at the point at which this steady state vanishes, the pheromone-only equilibrium becomes the stable attracting point. This either happens with a simple exchange of stability, or through a more complex route involving a Hopf bifurcation and a heteroclinic

cycle. In both cases, the transition to scent trails has been made at $N_{\max}$ (or earlier), rather than at N_3.

What may we infer about properties of the model for values of c_5 between 0 and c_6? For $0 < c_5 < c_6$ there are potentially two steady states involving group recruiters. For each of these, the numbers of GR and PT ants are given by

$$\bar{l} = N - \beta - \frac{\beta}{c_2} q_4(c_3 + q_4), \quad \bar{p} = \frac{\beta}{c_2} q_4(c_3 + q_4).$$

Recall from Section 3 that the scent trail at steady state satisfies

$$\gamma q_4^2 + (c_3\gamma - c_4)q_4 + c_5(N - \beta) = 0, \tag{20}$$

where, as before,

$$\gamma = \frac{\beta}{c_2}(c_6 - c_5).$$

Hence, we find two potential steady states for $\bar{q}$,

$$q_4 = \frac{c_4 - c_3\gamma}{2\gamma} - \frac{1}{2\gamma}\sqrt{(c_4 - c_3\gamma)^2 - 4c_5\gamma(N - \beta)},$$

and

$$q_5 = \frac{c_4 - c_3\gamma}{2\gamma} + \frac{1}{2\gamma}\sqrt{(c_4 - c_3\gamma)^2 - 4c_5\gamma(N - \beta)}.$$

These exist provided that

$$N < N_{\mathrm{SN}} = \beta + \frac{(c_3\gamma - c_4)^2}{4\gamma c_5}.$$

At $N = N_{\mathrm{SN}}$ a saddle-node bifurcation occurs at which the solutions disappear.

The analysis of the case $c_5 = c_6$ gives us a good indication of the expected stability properties of the mixed steady states for $c_5 \in (0, c_6)$. There are again two cases, depending on whether c_2 is smaller or greater than $c_2^* = \alpha^2\beta^2$.

If $c_2 > c_2^*$, then the family of mixed steady states intersects the P_2 branch in one value of N. The bifurcation occurring there is a transcritical one, an exchange of one stable eigenvalue. However, for small values of c_5, the branch of mixed steady states extends beyond $N = N_{\max}$, and there is a saddle-node bifurcation at the turning point $N = N_{\mathrm{SN}}$. This suggests that as N increases, the P_4 branch is followed beyond $N = N_{\max}$, and at the turning point the solution drops off the P_4 branch and converges to P_2. Numerical experiments agree with this, see Figure 4.

If $c_5 = c_6$ and $c_2 < c_2^*$, then we have seen that a Hopf bifurcation occurs for some value of N between $N_{\min}$ and $N_{\max}$. Numerical experiments suggest that this remains the case as long as the $q_4(N_{\mathrm{SN}}) > q_4(N_{\max})$. As c_5 decreases from c_6, this is certainly the case, and there is one value of c_5 at which $N_{\max} = N_{\mathrm{SN}}$. For c_5 less than this number, $N_{\mathrm{SN}} > N_{\max}$, but $q_4(N_{\mathrm{SN}}) < q_4(N_{\max})$. Figure 5 gives an illustration that the Hopf bifurcation extends for some range of c_5's, after which the behaviour is as in the previous case.

7. Discussion

7.1. **Main results.** We have modelled the dynamics of the growth of the populations of recruited foragers in colonies of ants in which the workers are able to employ two different recruitment methods, group recruitment (including tandem running; GR) and pheromone trails (PT). The main question we have posed is whether GR may aid in the establishment of trails when numbers of ants is small.

The model clearly shows that such is the case. When trails are not laid down by GR ants, colony size N has to be sufficiently large for solutions to converge to scent trail steady states. When GR ants do contribute, solutions generally converge to PT equilibria at lower colony sizes. Mathematically, this may happen in three ways: (1) through a simple exchange of stability in a transcritical bifurcation; (2) through a saddle-node bifurcation where GR equilibria cease to exist; (3) through a Hopf bifurcation combined with a subsequent heteroclinic cycle.

We have found two main cases. If probabilities to lose a trail are low, then colonies end up using both trails and group recruitment at smaller values of N, and exclusively trails for large values of N.

In the second case, if probabilities to lose a trail are high, then a moderate contribution to the trail by group recruiters allows colonies to show the same recruitment behaviour switching as when in the previous corresponding case. If group recruiters contribute equally to trails compared to trail following ants, then colonies are able to converge to exclusive use of pheromone trails at much smaller colony size, which mathematically happens by way of a Hopf bifurcation and subsequent heteroclinic cycle.

In summary, ant colonies for which scent trails are less efficient, for instance because their habitat does not promote long-lived trails, would benefit from a combined GR/PT recruitment system, allowing them to establish scent trails even at low colony sizes.

7.2. **Group-mass recruitment and collective decision making.** In addition to showing that small colonies can build succesful scent trails through initial group recruitment, it has also been demonstrated that this combined system gives colonies greater flexibility and speed in their choice of foraging sites. Once an initial choice has been made, a species with a combined recruitment system can change its decision by deploying subsequent group recruitment, whereas a species with only trails could not (Beckers et al., 1990).

Collignon and Detrain (2010) have provided experimental evidence that groups of recruits in *Tetramorium caespitum* are faster to form, are larger, and will recruit more reliably towards a food droplet with a higher energetic content in sugars.

In another species, *T. bicarinatum*, ants have been shown to be more willing to follow a leader to a new nest source in a GR event than merely to follow the trail laid by that same leader previously (de Biseau et al., 1994). One explanation for

this is that the probability to lose this weak trail is likely to be much greater than the probability to arrive at the food source through group recruitment.

The probability to lose this weak trail may be indeed greater than the probability to arrive at the food source through group recruitment. In *T. bicarinatum*, these groups are still seen even when a collective trail has been established, in contrast with other related species, such as *T. impurum*.

7.3. **The role of trail efficiency.** Throughout the paper we have focussed on the role of c_2 to determine which type of changes of stability occurred. This parameter has a relatively clear interpretation, as it is directly related to the probability to lose the scent trail. When trails work very well, c_2 is low, and when for instance, trails degrade quickly, c_2 is high. When scent marks work very well, there are in fact no mixed equilibria at all (inequality (6) is not satisfied). The minimum colony size necessary to reach the PT equilibria, N_3, is also small.

In the other case, however, there are stable mixed equilibria and the minimum colony size to reach PT equilibria is higher. Especially when GR ants contribute to trails just as much as PT ants do (which is most likely, since after all the same ants are involved in different tasks at different times), solutions definitely converge to a trail steady state when colony size has surpassed $N_{\max}$.

Since

$$\alpha^2\beta(N_{\max} - N_3) = (\alpha\beta - c_3)\Big(\alpha\beta - \frac{c_2}{c_3}\Big),$$

$N_{\max} < N_3$ when $c_3 < \alpha\beta$ and (6) are satisfied. These two inequalities are only met simultaneously if $c_3 < c_2/c_3$, i.e. when $c_2 > c_3^2$. The righthand side is minimized if $\alpha\beta$ lies inbetween c_3 and c_2/c_3. Hence, a combination of a low net deposition rate of trail scent (α low) and good GR recruitment build up (β high) should give the greatest benefit of GR to PT.

7.4. **Experimental evidence for an association between mixed recruitment methods and small colony sizes.** *Tetramorium caespitum* is one of the species in which the combined GR/PT recruitment system has been documented. Colonies start as single queens and grow to have worker populations between about 1,000-30,000 ants (Brian et al., 1965, 1967) with many colonies reaching about 10,000. As such, these colonies clearly undergo growth over three to four orders of magnitude. Our modelling suggests that the GR/PT recruitment system allows them to overcome potential growth obstacles by foraging efficiently at low colony sizes through the use of group recruitment to establish effective and reliable trails.

In Beckers et al. (1989), a distinction is made between group/mass recruitment, and other uses of trails which are called mass recruitment, trunk trails and group hunting. The median colony size for group/mass recruiting species is indeed lower than for the other mass recruitment strategies, as suggested by our model.

$N_{\min}$	β
$N_{\max}$	$\beta - \frac{c_3}{\alpha} + \frac{c_2}{\alpha^2\beta}$
N_{SN}	$\beta + \frac{(c_3\gamma - c_4)^2}{4\gamma c_5}$
N_3	$\frac{c_2}{\alpha c_3}$
N_H	Hopf occurs
$\hat{N}$	$\frac{1}{\alpha}(2\sqrt{c_2} - c_3)$
α	$\frac{c_6}{c_4}$
β	$\frac{c_8}{c_7}$
γ	$\frac{c_8}{c_2 c_7}(c_6 - c_5)$
c_2^*	$\alpha^2\beta^2$

TABLE 1. Important parameter values used in the paper.

7.5. **Modelling approach.** The model studied in this paper is deterministic. However, for small colony sizes stochastic effects might be important. At present, the literature offers little information on real colony sizes to guide us; the scant evidence available suggests that species a GR/PT recruitment system have mature colony sizes in the order of 10,000, which should be fine for deterministic models. We expect that a stochastic approach would allow for less analysis and thus a reduced understanding of the model than in the current deterministic framework. We also expect such a model would indicate that the transition from no recruitment through mixed GR-PT recruitment to PT recruitment would occur at somewhat higher colony sizes because of possible stochastically occurring failures in the build up of recruitment numbers. On average, however, both modelling approaches should give quite similar results.

7.6. **Conclusion.** One important question in the study of social insect behaviour is how the internal organization of colonies keeps up with colony growth spanning several orders of magnitude. In ants, bees and termites, recruitment systems have been shown to be powerful and flexible collective mechanisms to provide work forces where labour is needed. This study now shows that *combinations* of such methods may provide additional advantages, allowing them to use mass recruitment methods even in the absence of 'masses' of ants.

The study of growing social insect societies is still in its infancy. Robustness of mechanisms that can perform well over very substantial ranges of colony sizes and under varying environments are likely to play a pivotal role. Studies linking colony growth to internal colony organization should provide a much needed and deeper understanding of the ecological success of the social insects.

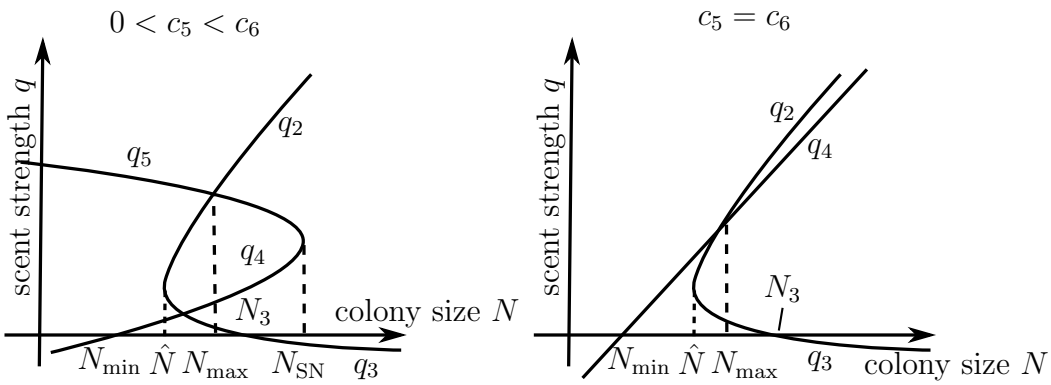

FIGURE 1. Schematic diagrams depicting the q-component of the various equilibria for varying colony size N, showing the relative positions of the critical values $N_{\min}$, $N_{\max}$, $\hat{N}$, N_3 and $N_{\rm SN}$. Left, a generic example in which $0 < c_5 < c_6$. The steady state P_4, corresponding with q_4 in the figure, is biologically relevant for $N \in [N_{\min}, N_{\rm SN}]$. Right, the case $c_5 = c_6$. The P_4 steady state is now biologically relevant for $N \in [N_{\min}, N_{\max}]$.

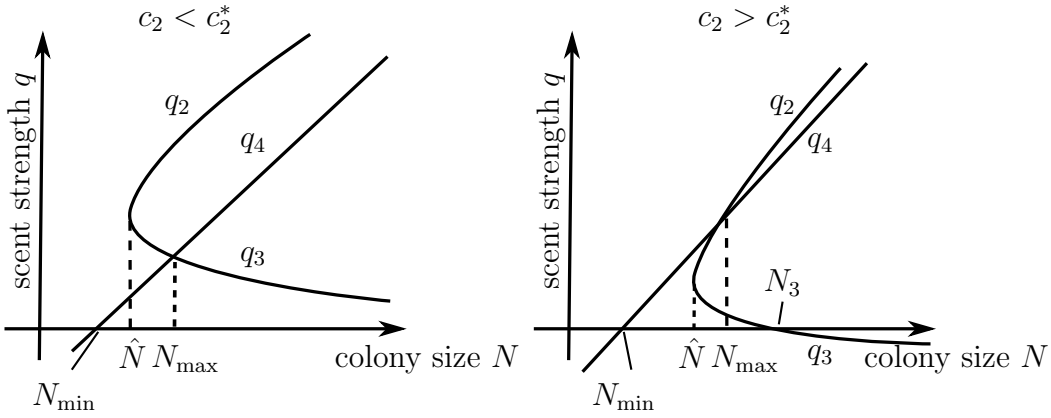

FIGURE 2. Schematic diagrams of the q-components of the equilibria for the model with $c_5 = c_6$. Left, $c_2 < c_2^*$ so that $q_4(\hat{N}) < q_2(\hat{N}) = q_3(\hat{N})$; right, $c_2 > c_2^*$, hence $q_4(\hat{N}) < q_2(\hat{N})$.

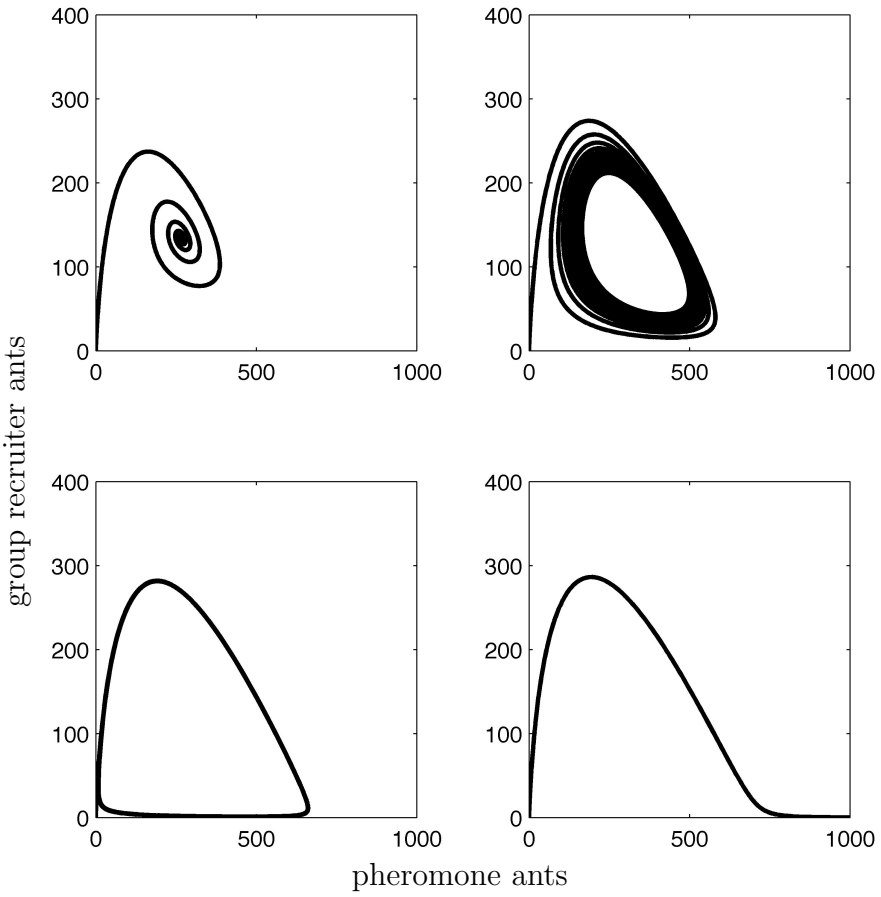

FIGURE 3. Example numerical runs of model (10)–(12) for colony sizes $N = 4400, 4460, 4473, 4480$, from left to right, top to bottom. Note the convergence to a stable mixed equilbrium in the first plot, followed by a Hopf bifurcation (top right), an orbit approaching a heteroclinic connection (bottom left), and finally a solution converging to the stable pheromone equilibrium on the P_2 branch (bottom right). Parameter values used are $c_2 = 3$, $c_3 = 0.1$, $c_4 = 10$, $c_6 = 0.01$, $c_7 = 0.01$, $c_8 = 40$.

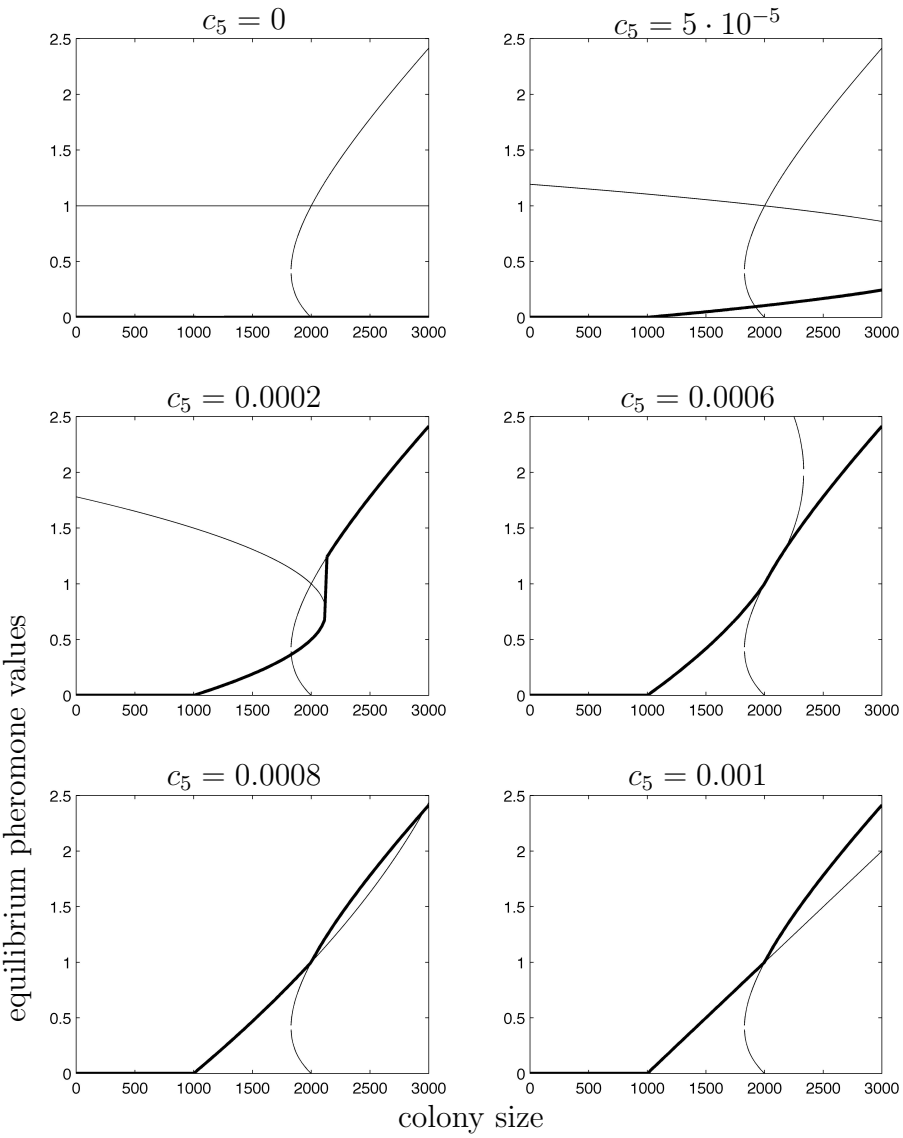

FIGURE 4. Connecting $c_5 = 0$ to $c_5 = c_6$. Rate constants are, $c_2 = 2$, $c_3 = 1$, $c_4 = 1$, $c_6 = 0.001$, $c_7 = 0.001$, $c_8 = 1$, and c_5 as indicated above the figures. Bold lines show long-term behaviour of solutions starting near the origin, thin lines the families of steady states. In this case $c_2 < c_2^*$. In all but the $c_5 = 0$ case, solutions starting near the origin converge to the mixed steady state for smaller values of N and to the scent-only steady state for large values of N. For small values of c_5, this transition occurs by means of a saddle-node bifurcation, and for large values of c_5 a transcritical bifurcation occurs.

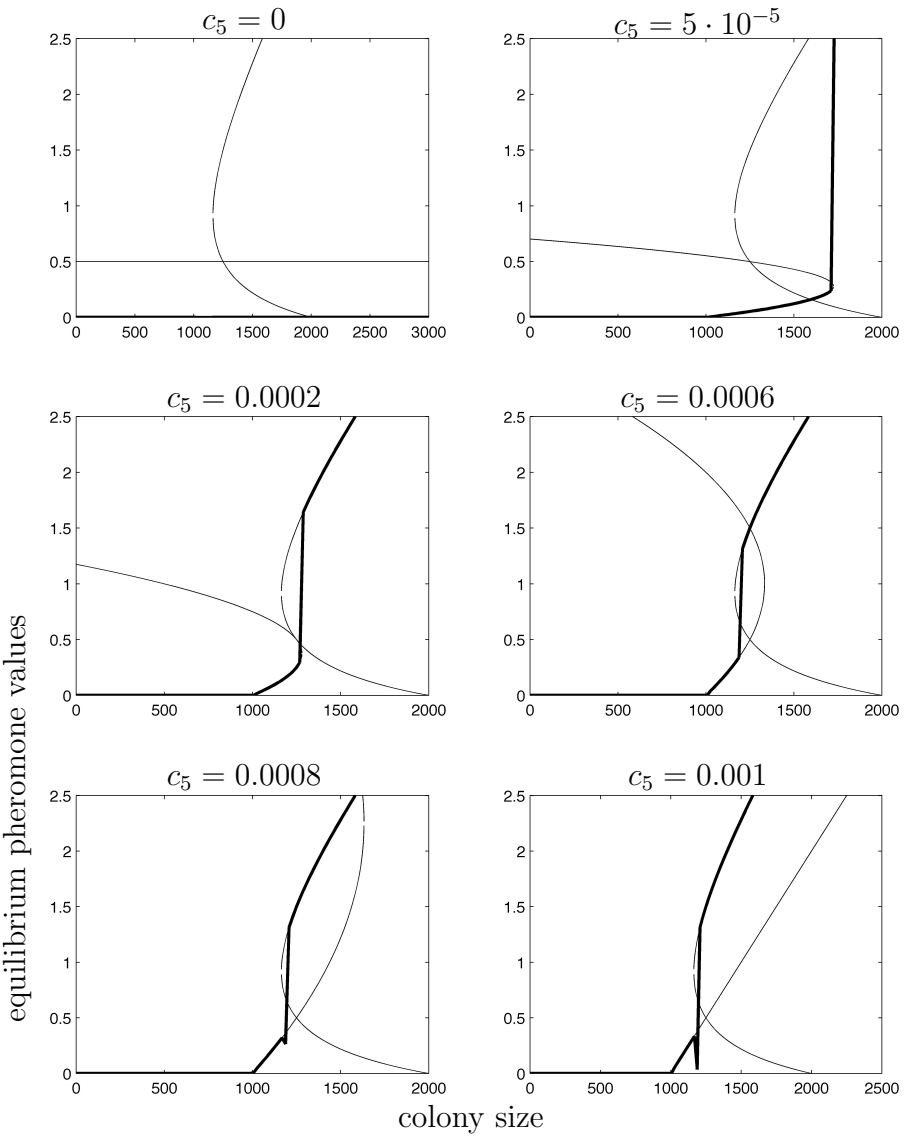

FIGURE 5. Connecting $c_5 = 0$ to $c_5 = c_6$. Rate constants are, $c_2 = 2$, $c_3 = 0.5$, $c_4 = 0.5$, $c_6 = 0.001$, $c_7 = 0.001$, $c_8 = 1$, and c_5 as indicated above the figures. Bold lines show long-term behaviour of solutions starting near the origin, thin lines the families of steady states. In this case, $c_2 > c_2^*$. For c_5 just above zero, solutions starting near the origin drop off the branch of equilibria involving both group recruitment and pheromone trails as colony size increases; for large colony size solutions converge to the steady state involving only pheromone trails. For large c_5, solutions converge to these scent steady states much earlier, and drop off the mixed equilibria through a Hopf bifurcation and subsequent heteroclinic cycle. The 'kink' in the last two images are solutions converging to a limit cycle, and indicate that a Hopf bifurcation has occurred.

8. Appendix

As we have seen, a Hopf bifurcation exists whenever $N_{\min} < N_{\max}$, provided that $\hat{N} < N_{\max}$. In this Appendix we study these extremal situations $N_{\min} \lesssim N_{\max}$ and $\hat{N} \lesssim N_{\max}$ using an asymptotic analysis. See Figure 6 for a sketch of both extremal situations, and Figure 7 for an illustration of the equilibrium solutions near $N_{\min} = N_{\max}$.

8.1. **Unfolding the orbit structure: $N_{\min} \lesssim N_{\max}$.** We start with $N_{\min} = N_{\max} = \beta$, which occurs precisely when

$$\frac{c_2}{c_3\alpha\beta} = 1,$$

and assume that the P_4 branch intersects P_3, which in this particular case is equivalent to requiring that $\hat{N} < N_{\min}$, or $c_2 > c_3^2$. Let us introduce a small parameter ε by setting

$$\varepsilon = \frac{c_2}{c_3\alpha\beta} - 1 \tag{21}$$

and introduce the rescaling

$$N = \beta + \varepsilon N^*,$$

where $N^* = \mathcal{O}(1)$. To be concrete, we write (21) in the form

$$c_6 = \frac{c_2c_4c_7}{c_3c_8(1+\varepsilon)}. \tag{22}$$

We substitute a power series expansion of the variables, given by

$$p(t) = p_0(t) + \varepsilon p_1(t) + \varepsilon^2 p_2(t) + \cdots, \tag{23}$$

$$q(t) = q_0(t) + \varepsilon q_1(t) + \varepsilon^2 q_2(t) + \cdots, \tag{24}$$

$$l(t) = l_0(t) + \varepsilon l_1(t) + \varepsilon^2 l_2(t) + \cdots. \tag{25}$$

into the equations (10)–(12), and change the time scale by setting $\tau = \varepsilon t$. (Note that the p_i, q_i and l_i have nothing to do with their previous use in equilibria $P_1, \ldots, P_5$.) The $\mathcal{O}(\varepsilon^0)$ problem is then simply the set of steady state equations for p_0, q_0 and l_0. Since we are expanding near the origin, we conclude $p_0 = q_0 = l_0 = 0$. The $\mathcal{O}(\varepsilon)$ problem in time τ is given by

$$\begin{aligned} 0 &= q_1\frac{c_8}{c_7} - p_1\frac{c_2}{c_3}, \\ 0 &= -c_4q_1 + (l_1 + p_1)\frac{c_2c_4c_7}{c_3c_8}, \\ 0 &= l_1. \end{aligned}$$

We thus find that the first two equations both give

$$q_1 = \frac{c_2 c_4 c_7}{c_3 c_8} p_1. \tag{26}$$

The order ε^2 problem is

$$\frac{dp_1}{d\tau} = q_1(N^* - p_1) + \frac{c_8}{c_7} q_2 - \frac{c_2 p_2 - \frac{c_2}{c_3} p_1 q_1}{c_3}, \tag{27}$$

$$\frac{dq_1}{d\tau} = -c_4 q_2 + \frac{c_2 c_4 c_7}{c_3 c_8}(l_2 + p_2 - p_1), \tag{28}$$

$$\frac{dl_1}{d\tau} = 0. \tag{29}$$

Substituting equation (26) into the second equation (28), we can solve for q_2 and substitute into the first equation (27). The p_2 terms cancel, and we are left with

$$\frac{dp_1}{d\tau} = \frac{c_2 c_4 c_7}{c_3^3(c_8 + c_4 c_7)} \left(c_7(c_3^2 - c_2)p_1^2 + c_3^2(c_7 N^* - c_8)p_1 + c_3^2 l_2 \right). \tag{30}$$

Together with the order ε^3 equation for l_2,

$$\frac{dl_2}{d\tau} = c_7 l_2 (N^* - p_1), \tag{31}$$

equations (30) and (31) for p_1 and l_2 form a closed set of equations. This set of equations has three equilibria. First the origin, second, a pheromone-only steady state

$$(\bar{p}_1, \bar{l}_2) = \left(\frac{c_3^2(c_8 - c_7 N^*)}{c_7(c_2 - c_3^2)}, 0 \right),$$

which is biologically relevant when $c_2 > c_3^2$, which we assumed at the start of this section, and when $N^* < \frac{c_8}{c_7} = \beta$. This steady state is the part of the family of P_{23} equilibria close to the origin, and thus remains in this scaling. Third, we find a mixed steady state,

$$(\hat{p}_1, \hat{l}_2) = \left(N^*, N^* \left(1 - \frac{c_2 c_7}{c_3^2 c_8} N^* \right) \right)$$

This steady state exists for $N^* \in [0, \frac{c_3^2}{c_2}\beta]$. Note that $\frac{c_3^2}{c_2}\beta < \beta$ since $c_3^2 < c_2$ by assumption.

How much of the dynamics of the full three-dimensional system can be recovered in this two-dimensional system? First, we can recover the Hopf bifurcation occurring between $N^* = 0$ and $N^* = \frac{c_3^2}{c_2}\beta$. The Jacobian at this mixed steady is

$$J = \begin{pmatrix} \frac{c_2 c_4 c_7}{c_3^3 c_8 (c_4 c_7 + c_8)}(c_7 N^*(2c_2 - c_3^2) - c_3^2 c_8) & \frac{c_2 c_4 c_7}{c_3(c_4 c_7 + c_8)} \\ \frac{c_7 N^*(c_7 N^* c_2 - c_3^2 c_8)}{c_3^2 c_8} & 0 \end{pmatrix}.$$

The conditions for a Hopf bifurcation are tr $J = 0$ and det $J > 0$. The value of N^* at which the trace becomes zero is

$$N^* = \beta \frac{c_3^2}{2c_2 - c_3^2} = \beta \frac{c_3^2}{c_2 + (c_2 - c_3^2)} < \beta \frac{c_3^2}{c_2}.$$

It is easy to check that the determinant remains positive at the above value of N^*.

The heteroclinic cycle does appear in this scaling. To find it, we study the 2D system more abstractly. Equations (30)-(31) have the form

$$\frac{dp}{dt} = Ap(p - B) + Cl, \tag{32}$$

$$\frac{dl}{dt} = Dl(N^* - p), \tag{33}$$

for suitable positive constants A, B, C and D. Whenever the pheromone-only steady state $(\bar{p}, 0)$ exists, there also exists an orbit connecting it with the origin, through the p-axis. We now show that for a particular choice of N^* there also exists an orbit connecting the orbit with $(\bar{p}, 0)$ forward in time. For a particular value of B, this system has solutions symmetric about $u = N$, namely for $B = 2N^*$: then the term $Ap(p - 2N^*)$ is symmetric about the $p = N^*$ line. For this particular choice of B we can find a function which is conserved along orbits. Write

$$\frac{dl}{dp} = \frac{Dl(p)(N^* - p)}{Ap(p - 2N^*) + Cl(p)},$$

and solve for $l(p)$ (directly, using Maple) to find

$$M(p, l) := Dl^{2A/D} \left(\frac{1}{2} p(p - 2N^*) + \frac{CDl}{2A + D} \right) = \text{constant}. \tag{34}$$

The zero level set yields

$$l = 0, \quad l = \frac{2A + D}{2CD} p(2N^* - p).$$

The latter is a parabola connecting $(p, l) = (0, 0)$ to $(p, l) = (2N, 0)$. The two orbits connecting $(\bar{p}, 0)$ and the origin form a heteroclinic cycle. For level sets above zero, we find a set of nested periodic orbits centered on the mixed steady state $(\hat{p}_1, \hat{l}_2)$, see Figure 8. Finally, using the full equation for p_1 (30), note that $B = 2N^*$ means that

$$N^* = B/2 = N^*_{\text{Hopf}} = \beta \frac{c_3^2}{2c_2 - c_3^2}.$$

Hence, the Hopf bifurcation occurs at the same value of N^* as the heteroclinic orbit.

We can also show that $N^* = B/2$ is the only value of N^* at which periodic orbits and the heteroclinic cycle exist. We treat the case $B > 2N^*$; the argument for $B < 2N^*$ is a straightforward extension.

Let us thus assume that $B > 2N^*$. Local stability analysis shows that the mixed equilbrium is locally stable in this case. The result follows from the following monotonicity property. Let Q be any point on the l-isocline above the equilibrium: $Q = (N^*, \bar{l})$. Consider the orbit with initial data Q. The forward orbit is described by the graph $p = \phi_+(l)$, the backward orbit by $p = \phi_-(l)$, at least until the orbits hit the l-isocline again. Note that $\phi_+(l) > \phi_\pm(\bar{l}) = N^* > \phi_-(l)$ for $l < \bar{l}$.

The flow lines are determined by

$$\frac{d\phi_\pm}{dl} = G(\phi_\pm(l), l), \tag{35}$$

with

$$G(p, l) = \frac{Ap(p - B) + Cl}{Dl(N^* - p)}.$$

Now reflect the orbit $p = \phi_-(l)$ in the l-isocline: $p = \phi^*_-(l) = 2N^* - \phi_-(l)$. Then

$$\frac{d\phi^*_-}{dl} = G^*(\phi^*_-(l), l), \tag{36}$$

with

$$G^*(p, l) = G(2N^* - p, l).$$

Since $B > 2N^*$, we infer that

$$G^*(p, l) < G(p, l) \quad \text{for all } p < N^*.$$

Hence, (35) and (36) now imply that $\phi_+(l) < \phi^*_-(l)$ by usual ODE techniques. Using standard phase-plane arguments, one finds for example that that no periodic orbit exists, and that the orbit forming the unstable manifold of the origin spirals towards the nontrivial equilibrium.

For $B < 2N^*$, the origin remains unstable, as is now the nontrivial equilibrium. All orbits now tend to infinite p while l vanishes.

8.2. **Unfolding the orbit structure: $\hat{N} \lesssim N_{\max}$.** We now consider the other extremal situation, where the Hopf bifurcation ceases to exist: $\hat{N} = N_{\max}$ (see Figure 6). We conjecture that the heteroclinic cycle remains as $\hat{N}$ approaches $N_{\max}$, but it is not to be expected that asymptotic analysis reveals this: the heteroclinic cycle consists of orbits connecting the origin and a steady state far removed from the origin. Expanding solutions around this second steady state, we will not be able to find those heteroclinic orbits. (In the first extremal case, the second steady state *was* situated close the origin, and the heteroclinic cycle was present in the asymptotic expansion.) Nevertheless, performing expansions still reveals much of the structure of solutions close to the point where $\hat{N} = N_{\max}$, in particular the distance between N_h and $N_{\max}$ as $\epsilon \to 0$.

One way to characterize $\hat{N} = N_{\max}$ is by choosing $c_2 = c_2^* = \alpha^2\beta^2$, so that $\hat{N} = N_{\max} = 2\beta - c_3/\alpha$. Performing an asymptotic expansion as in the first case is now more subtle. We introduce a small parameter ε by setting

$$c_2 = \alpha^2\beta^2(1-\varepsilon). \tag{37}$$

Next, both $\hat{N}$ and $N_{\max}$ will change when we vary ε, and the distance between these two points is of order ε^2. It is to be expected from (19) that for $\varepsilon > 0$ small, the Hopf bifurcation appears at some value of N_H close to $N_{\max}$, but it turns out that it occurs at a distance of order ε, not ε^2, as we will show later on. Hence, when performing the asymptotic expansion using $N = 2\beta - c_3/\alpha + \varepsilon^2 N^*$, we find in timescale $\tau = \varepsilon t$ solutions which do not undergo any Hopf bifurcation.

The direct approach of studying the eigenvalues near $\hat{N} = N_{\max}$ is more fruitful. Next to (37), we set

$$N = 2\beta - \frac{c_3}{\alpha} + \varepsilon N^*.$$

We compute the Jacobian matrix of our original system of equations, and substitute the branch of mixed equilibria P_4, along which the Hopf bifurcation should occur. The resulting eigenvalue equation is of the form

$$Q_0(\varepsilon) + Q_1(\varepsilon)\lambda + Q_2(\varepsilon)\lambda^2 + \lambda^3 = 0,$$

for suitable functions Q_0, Q_1, Q_2. In $\varepsilon = 0$, there is a double root $\lambda = 0$ and one negative root $\lambda_1 < 0$. Hence, we can write the above equation as

$$(\lambda - \lambda_1(\varepsilon))(R_0(\varepsilon) + R_1(\varepsilon)\lambda + \lambda^2) = 0,$$

where $\lambda_1(0) < 0$, and R_0 and R_1 are suitable functions satisfying $R_0(0) = R_1(0) = 0$. We are only interested in the case when $R_0 = A\varepsilon + \mathcal{O}(\varepsilon^2)$, with $A > 0$, since we want to find complex eigenvalues. To lowest order then, the second factor is of the form $\lambda^2 + B\varepsilon\lambda + A\varepsilon = 0$, from which we conclude that the imaginary part of these complex eigenvalues are of order $\sqrt{\varepsilon}$, and the real part is of order ε. To find the Hopf bifurcation, we thus substitute $\lambda = i\sqrt{\varepsilon}\mu$ into the eigenvalue equation, and separate imaginary and real parts. We find that μ and N^* must satisfy the following two linear equations,

$$S_1\mu^2 + S_2 N^* = 0, \tag{38}$$

$$\mu^2 + S_3 N^2 = S_4, \tag{39}$$

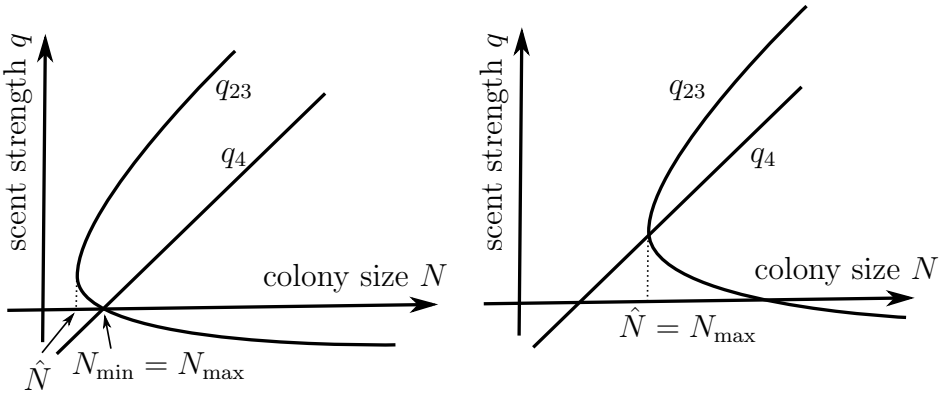

FIGURE 6. The two extremal situations where the Hopf bifurcation appears and vanishes. Left, $N_{\min} = N_{\max}$, characterized by $\alpha\beta c_3 = c_2$; right, $\hat{N} = N_{\max}$, which occurs when $c_2 = c_2^* = \alpha^2\beta^2$.

where

$$\begin{aligned} S_1 &= c_3 - 2\alpha\beta - c_4, \\ S_2 &= c_4 c_7 (c_3 - \alpha\beta), \\ S_3 &= \frac{c_7}{c_4}\Big(\frac{c_3}{c_4} - 1 + \frac{c_3}{\alpha\beta}\Big) - \frac{c_3}{\beta} - \frac{c_8 c_6}{c_4^2}, \\ S_4 &= \frac{c_3 - \alpha\beta}{c_4}. \end{aligned}$$

Inequality (6) and the specific choice of c_2 may be combined to infer that $c_3 < (1-\epsilon)\alpha\beta$. Therefore, S_1, S_2 and S_4 are all negative.

Writing out the α's and β's in S_3, and then collecting terms to produce a polynomial in c_7, we get

$$S_3 = \frac{c_4^2 c_3}{c_6 c_8} c_7^2 + \Big(- c_4 - \frac{c_4 c_3}{c_8} + c_3 \Big) c_7 - \frac{c_6 c_8}{c_4}. \tag{40}$$

The restriction $0 < c_3 < \alpha\beta$ can be rewritten as $0 < c_7 < c_6 c_8 / c_3 c_4$. On this interval $S_3 < 0$ as a function of c_7, since it is negative in both end points of the interval.

Finally, directly solving the two linear equations yields

$$\mu^2 = \frac{S_2 S_4}{S_1 S_3 - S_2} > 0, \quad N^* = -\frac{S_1 S_4}{S_1 S_3 - S_2} = -\frac{S_1}{S_2}\mu^2 < 0$$

This completes the proof that a Hopf bifurcation occurs at a distance of order ε from $N_{\max}$. (It was to be expected that $N^* < 0$, since we expect the value of N to be less than $N_{\max}$, and we have set $N = N_{\max} + \varepsilon N^*$.)

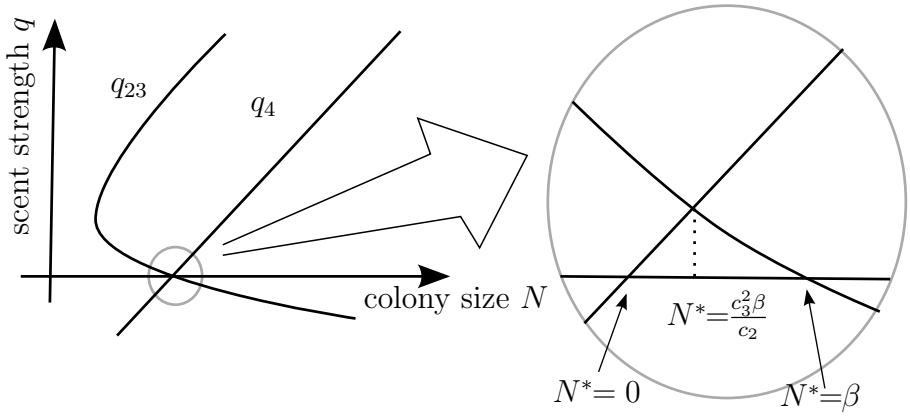

FIGURE 7. Schematic bifurcation diagram of model (10)–(12), in the case when $N_{\max} = N_{\min} + \varepsilon N^*$ with ε small but positive. The figure in the circle on the right gives an impression of the steady states close to the origin and which are still captured by the asympotic expansion.

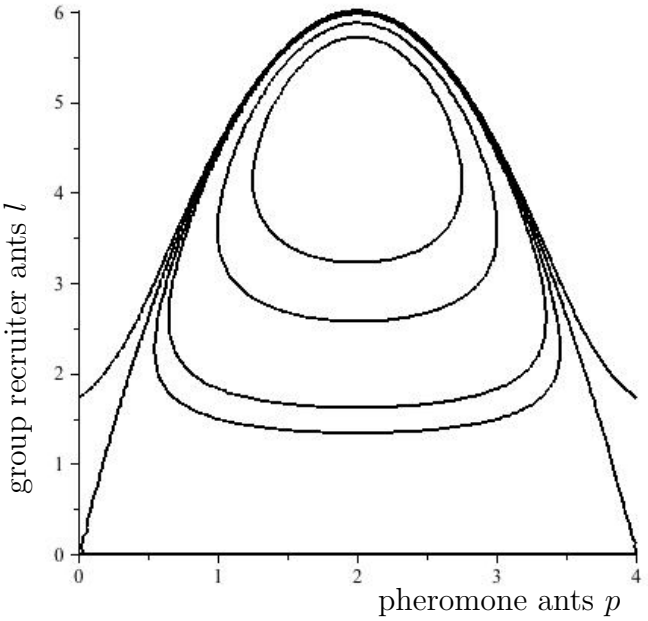

FIGURE 8. Example contours for the conserved quantity $M(p, l) =$ constant given by (34). Parameters were $A = 2$, $B = 4$, $C = 2$, $D = 2$, $N^* = 2$. Contours are plotted for levels $-10, 0, 10, 20, 100, 200$, from outside to inside. The two parts of the level 0 contour together form a heteroclinic connection.

References

Beckers, R., Deneubourg, J. L., Goss, S., and Pasteels, J. M. (1990). Collective decision making through food recruitment. *Insectes Soc.*, 37(3):258–267.

Beckers, R., Goss, S., Deneubourg, J. L., and Pasteels, J. M. (1989). Colony size, communication and foraging strategy. *Psyche*, 96:239–256.

Beekman, M., Sumpter, D. J. T., and Ratnieks, F. L. W. (2001). Phase transition between disorganised and organised foraging in Pharaoh's ants. *Proc. Nat. Acad. Sciences*, 98:9703–9706.

Bourke, A. F. G. and Franks, N. R. (1995). *Social evolution in ants*. Princeton University Press, Princeton, NJ.

Brian, M. V., Elmes, G., and Kelley, A. F. (1967). Populations of the ant *Tetramorium caespitum* Latreille. *J. Anim. Ecology*, 36(2):337–342.

Brian, M. V. and Elmes, G. W. (1974). Production by the ant *Tetramorium caespitum* in a Southern English heathland. *J. Anim. Ecology*, 43:889–903.

Brian, M. V., Hibble, J., and Stradling, D. J. (1965). Ant pattern and density in a Southern English heath. *J. Anim. Ecology*, 35(2):545–555.

Britton, N. F., Strickland, T. R., and Franks, N. R. (1998). Analysis of ant foraging algorithms. *J. Biol. Syst.*, 6:315–336.

Buschinger, A. (1974). Monogynie und Polygynie in Insektsozietäten. In Schmidt, G. H., editor, *Sozialpolymorphismus bei Insekten*, pages 862–896. Wissenschaftliche Verlagsgesellschaft MBH, Stuttgart.

Collignon, B. and Detrain, C. (2010). Distributed leadership and adaptive decision-making in the ant *Tetramorium caespitum*. *Proc. Roy. Soc. London B*, 277:1267–1273.

Couzin, I., Krause, J., Franks, N. R., and Levin, S. A. (2005). Effective leadership and decision-making in animal groups on the move. *Nature*, 433:513–516.

de Biseau, J. C., Schuiten, M., Pasteels, J. M., and Deneubourg, J. L. (1994). Respective contributions of leader and trail during recruitment to food in *Tetramorium bicarinatum* (Hymenoptera: Formicidae). *Insectes Soc.*, 41(3):241–254.

Dechaume-Moncharmont, F.-X., Dornhaus, A., Houston, A. I., McNamara, J. M., Collins, E. J., and Franks, N. R. (2005). The hidden cost of information in collective foraging. *Proc. Roy. Soc. London B*, 272:1689–1695.

Deneubourg, J., Pasteels, J., and Verhaeghe, J. (1983). Probabilistic behaviour in ants: A strategy of errors? *J. Theor. Biology*, 105(2):259–271.

Franks, N. R., Gomez, N., Goss, S., and Deneubourg, J. L. (1991). The blind leading the blind in army ant raid patterns: testing a model of self-organization. *J. Insect Behav.*, 4(5):583–607.

Haldane, J. B. S. and Spurway, H. (1954). A statistical analysis of communication in *Apis mellifera* and a comparison with communication in other animals. *Insectes Soc.*, 1:247–283.

Harrington, F. H. and Mech, L. D. (1979). Wolf howling and its role in territory maintenance. *Behaviour*, 68:207–249.

Hölldobler, B. and Wilson, E. O. (1977). The number of queens: an important trait in ant evolution. *Naturwissenschaften*, 64:8–15.

Hölldobler, B. and Wilson, E. O. (1990). *The Ants*. Belknap, Harvard, Cambridge, Massachussets.

Hölldobler, B. and Wilson, E. O. (2009). *The Superorganism: the beauty, elegance, and strangeness of insect societies*. W. W. Norton & Company, Inc.

Jackson, D. E., Martin, S. J., Holcombe, M., and Ratnieks, F. L. (2006). Longevity and detection of persistent foraging trails in Pharaohs ants, *Monomorium pharaonis* (L.). *Anim. Behav.*, 71:351–359.

Jackson, D. E. and Ratnieks, F. L. (2006). Communication in ants. *Current Biology*, 16(15):R570–R574.

Katzir, G. (1981). Aggression by the damselfish *Dascyllus aruanus* l. towards conspecifics and heterospecifics. *Anim. Behav.*, 29:835–841.

Oster, G. F. and Wilson, E. O. (1978). *Caste and ecology in the social insects*. Princeton University Press, Princeton, New Jersey.

Planqué, R., van den Berg, J. B., and Franks, N. R. (2010). Recruitment strategies and colony size in ants. *PLoS ONE*, 5:e11664.

Robinson, E. J. H., Jackson, D. E., Holcombe, M., and Ratnieks, F. L. (2005). 'No entry' signal in ant foraging. *Nature*, 438:442.

Tayssedre, C. and Moller, P. (1983). The optomotor response in weakly electrical fish. *Z. Tierpsychol.*, 60:265–352.

von Frisch, K. (1967). *The dance language and orientation of bees*. Cambridge: Harvard University Press.

Wilson, E. O. (1971). *The Insect Societies*. Belknap, Harvard, Cambridge, Massachussets.

Wilson, E. O. (1975). *Sociobiology: the new synthesis*. Harvard University Press, Cambridge, Massachussetts.

Department of Mathematics, VU University Amsterdam, Amsterdam, The Netherlands

E-mail address: r.planque@vu.nl

Department of Mathematics, VU University Amsterdam, Amsterdam, The Netherlands

School of Biological Sciences, University of Bristol, Bristol, UK